Eur. Phys. J. B **19**, 583–587 (2001)

THE EUROPEAN PHYSICAL JOURNAL B

EDP Sciences

Reaction-diffusion system with self-organized critical behavior

R. Pastor-Satorras[1,a] and A. Vespignani[2]

[1] Dept. de Física i Enginyeria Nuclear, Universitat Politècnica de Catalunya, Campus Nord, Mòdul B4, 08034 Barcelona, Spain
[2] The Abdus Salam International Centre for Theoretical Physics (ICTP), PO Box 586, 34100 Trieste, Italy

Received 16 November 2000

Abstract. We describe the construction of a conserved reaction-diffusion system that exhibits self-organized critical (avalanche-like) behavior under the action of a slow addition of particles. The model provides an illustration of the general mechanism to generate self-organized criticality in conserving systems. Extensive simulations in $d = 2$ and 3 reveal critical exponents compatible with the universality class of the stochastic Manna sandpile model.

PACS. 05.70.Ln Nonequilibrium and irreversible thermodynamics – 05.65.+b Self-organized systems

Since the introduction of the Bak, Tang, and Wiesenfeld sandpile model [1], the concept of self-organized criticality (SOC) [2] has witnessed a real explosion of activity, covering both the description of new models and the proposal of several theoretical approaches, aiming at an understanding of SOC phenomena in terms of standard statistical mechanical concepts. At this respect, it has been shown that SOC in sandpile models is related to the behavior of absorbing-state phase transitions (APT) with many absorbing states [3,4]. Indeed, this very idea is underlying a recipe proposed for the construction of SOC models [5]: any cellular automata, defined with *conserved* microscopic rules, and possessing many absorbing states, will display SOC behavior if *slowly driven* with the addition of energy/particles at a rate h and dissipation at a rate ϵ: *i.e.*, in the double limit $h \to 0$, $\epsilon \to 0$, with $h/\epsilon \to 0$ [6]. This mechanism is easily seen at work in all standard sandpile models proposed so far [1,7,8].

Given that most SOC systems are defined in terms of sandpile-like models (with the exception of the forest-fire [9] and extremal [10] models), it becomes all the most interesting to explore the possibility of applying the recipe of reference [5] to models of a qualitatively different sort. In this paper we consider a reaction-diffusion (RD) model showing an APT that conserves the total number of particles [11,12]. This model exhibits a non-equilibrium phase transition in the same universality class of fixed energy stochastic sandpiles [4,12]. Here, we show that implementing the slow driving condition, the model reaches a stationary state with an avalanche-like reaction activity with critical properties. By measuring usual magnitudes characterizing the SOC behavior, we compare the model with standard slowly driven sandpiles. The critical exponents measured confirm the shared universality class with stochastic sandpiles, and provide a vivid illustration of the SOC generating mechanism [5].

We focus on the two species RD system [11,12], recently proposed to describe APT coupled to a non-diffusive conserved field [13]. The RD system is defined by the following set of reaction steps:

$$B \to A \quad \text{with rate } k_1, \tag{1}$$

$$B + A \to 2B \quad \text{with rate } k_2. \tag{2}$$

In this system, B particles diffuse with diffusion rate D_B, and A particles *do not diffuse*, that is, $D_A = 0$. From the rate equations (1) and (2), it is clear that the dynamics conserves the total number of particles $N = N_A + N_B$, where N_i is the number of particles $i = A, B$. In this model, the dynamics is exclusively due to B particles, that we identify as *active* particles. A particles do not diffuse and cannot generate spontaneously B particles. More specifically, A particles can only move *via* the motion of B particles that later on transform into A through equation (2). This implies that any configuration devoid of B particles is an absorbing state in which the system is trapped forever. The number of these absorbing states is infinite – in the thermodynamic limit – corresponding to all the possible redistributions of N particles of type A in the system. This RD process exhibits a phase transition from an active phase (with an everlasting activity of B particles) to an absorbing phase (no B particles) for a critical value $\rho = \rho_c$ of the total particle density [12].

Here, we define a driven-dissipative version of the RD model by applying the recipe of references [4,5]. On hypercubic lattices of size L with open boundary conditions, each site i stores a number a_i of A particles and b_i of B particles. The occupation numbers a_i and b_i can have any integer value, including $a_i = b_i = 0$, that is, void sites with no particles. The model is thus representing the

[a] e-mail: romu@complex.upc.es

dynamics of *bosonic* particles. The initial configuration is constructed by randomly distributing a number N_0 of A particles in the lattice. The initial occupation numbers a_i have a Poissonian distribution, while $b_i = 0, \forall i$. Any configuration is stable whenever it fulfills this condition, *i.e.*, in the absence of B particles. The system is driven by adding one B particle to a randomly chosen site. A state with at least one B particle is called active. Active states evolve in time according to the following update rules, that mimic the diffusion and reaction steps in the RD system: I) Diffusion: on each lattice site, each B particle moves into a randomly chosen nearest neighbor site with probability $2d/(2d+1)$, and stays in the same site with probability $1/(2d+1)$; this results in an effective diffusivity $D_B = 1/(2d+1)$. II) After all sites have been updated for diffusion, we perform the reactions: a) On each lattice site, each B particle is turned into an A particle with probability r_1. b) At the same time, each A particle becomes a B particle with probability $1-(1-r_2)^{b_i}$, where b_i is the total number of B particles in that site. This corresponds to the average probability for an A particle of being involved in the reaction (2) with any of the B particles present on the same site. The probabilities r_1 and r_2 are related to the reaction rates k_1 and k_2 defined in equations (1) and (2). In general, we have that $r_i(k_i = 0) = 0$, $r_i(k_i = \infty) = 1$, and r_i is an increasing function of k_i. The analytic expression of r_i as a function of k_i is presumably quite complex and nontrivial. However, as we will argue later, the knowledge of the precise relationship between r_i and k_i is not necessary, since the critical behavior of the model should be independent of the exact values of the parameters r_i selected. B particles on boundary sites may choose to diffuse out of the lattice. In this case, the particle is removed out of the system, contributing to the dissipation. The system is updated in parallel until there are no more B particles and it is again in an absorbing state. During the dynamic evolution, the addition of new B particles is suspended; this of course corresponds to the slow-driving condition. The sequence of updates in the system (from the time we introduce a new B particle until a stable state is reached) is interpreted as an avalanche. We characterize avalanches by their size s and their duration t. The size of an avalanche is defined as the number of B particles present in the system at each time step, summed over all the parallel updates required to reach a new stable state. The duration of an avalanche is defined as the total number of parallel updates performed during the avalanche. In the slow driving perspective, the existence of a critical stationary state is easily understood. Particles are added only in the absence of activity ($\rho < \rho_c$), while dissipation acts only during activity ($\rho > \rho_c$). This implies that $\partial_t \rho$ always drives the system toward ρ_c, that in the thermodynamic limit is the only possible stationary value of the density [4,5].

We have performed numerical simulations of this model in dimensions 2 and 3, with system sizes ranging from $L = 64$ to $L = 1024$ in $d = 2$, and from $L = 74$ to $L = 280$ in $d = 3$. The reaction rates r_i reported here are $r_1 = 0.3$ and $r_2 = 0.4$ in $d = 2$, and $r_1 = 0.4$ and $r_2 = 0.5$ in $d = 3$; the numerical results however, are independent of the particular values of the reaction rates r_i employed. The independence of the dynamics from the particular parameters r_i chosen can be easily grasped by the mean-field approach reported in reference [11], that shows the existence of a single critical point. More precisely, this can be understood in terms of renormalization-group arguments: The critical behavior of the model is ruled by the fixed point toward which the parameters flow under an appropriate renormalization-group transformation [11]. Thus, the critical exponents are independent of the initial values of the parameters, and depend only on the value of the unique fixed point. It is then natural that simulations performed with different r_i parameters will yield the same steady state behavior. This fact is confirmed by the numerical simulations, which show differences only in the transient regime. After the transient initial regime (whose length depends on L, r_i, and the initial concentration N_0 of A particles), the system reaches a steady state in which the stable configurations have a constant average number $\bar{N}_A$ of A particles and avalanches have a constant average size $\langle s \rangle$. As an example, in Figure 1, we plot the number of A particles and the average avalanche size as a function of the number of avalanches T in a simulation with system size $L = 256$ in $d = 2$, starting from an empty lattice. In analogy with sandpiles and SOC phenomena, in the steady state, we compute the probability distribution of sizes $P(s)$ and times $P(t)$ for the reaction events. By assuming the usual finite-size scaling form (FSS) [14]

$$P(s, L) = s^{-\tau_s} \mathcal{F}\left(\frac{s}{L^D}\right), \tag{3}$$

$$P(t, L) = t^{-\tau_t} \mathcal{G}\left(\frac{t}{L^z}\right), \tag{4}$$

we can define the standard critical exponents, τ_s, τ_t, D (the fractal dimension), and z (the dynamic critical exponent), which characterize the universality class of the

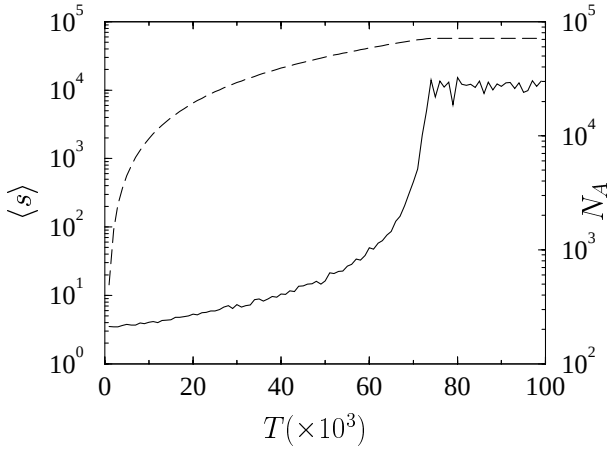

Fig. 1. Number of A particles N_A (dashed line) and average avalanche size $\langle s \rangle$ (full line) as a function of the number of avalanches T in a slowly driven conserved reaction diffusion system in a lattice of size $L = 256$. The initial state is an empty lattice.

Table 1. Critical exponents for the conserved RD and the stochastic Manna models in $d = 2$. Figures in parenthesis indicate the statistical uncertainty in the last digit. Manna exponents from references [17–20].

	τ_s	D	τ_t	z
Conserved RD	1.28(1)	2.75(1)	1.50(2)	1.54(1)
Manna	1.28(1)	2.76(1)	1.48(2)	1.55(1)

Table 2. Critical exponents for the conserved RD and the stochastic Manna models in $d = 3$. Figures in parenthesis indicate the statistical uncertainty in the last digit.

	τ_s	D	τ_t	z
Conserved RD	1.42(1)	3.36(1)	1.80(2)	1.77(1)
Manna	1.41(1)	3.36(1)	1.78(2)	1.76(1)

model. Averages are performed over at least 5×10^6 avalanches in $d = 2$. The distributions on $d = 3$ are considerably noisier; averages have thus been done in this case over 10^7 avalanches. In order to check the plausibility of the FSS hypothesis (3) and (4), and compute the corresponding critical exponents, we have applied the moment analysis technique, introduced in reference [15]. We define the q-th moment of the avalanche size distribution on a lattice of size L as $\langle s^q \rangle_L = \int \mathrm{d}s\, s^q\, P(s, L)$. If the FSS hypothesis (3) is valid in the asymptotic limit of large s, then the q-th moment has the following dependence on system size:

$$\langle s^q \rangle_L = L^{D(q+1-\tau_s)} \int \mathrm{d}y\, y^{(q-\tau_s)}\, \mathcal{F}(y) \sim L^{\sigma_s(q)}. \qquad (5)$$

The exponent $\sigma_s(q) = D(q + 1 - \tau_s)$ is computed as the slope of the log-log plot of $\langle s^q \rangle_L$ as a function of L. For large enough values of q (*i.e.*, away from the region where the integral in (5) is dominated by its lower cut-off), one can compute the fractal dimension D as the slope of $\sigma_s(q)$ as a function of q: $D = \partial\sigma_s(q)/\partial q$. Once D is known we can estimate τ_s using the relation $\sigma_s(1) = D(2 - \tau_s)$. The exponent $\sigma_s(1)$, giving the scaling of the average avalanche size, can be estimated using a standard argument in sandpiles: a new injected particle B performs a diffusing Brownian motion and has to travel, on average, a distance of order L^2 before reaching the boundary. In the stationary state, to each B particle drop must correspond, on average, a B particle diffusing out of the system. This implies that the average avalanche size corresponds to the average number of diffusion steps needed for a B particle to reach the boundary; *i.e.*, $\langle s \rangle \sim L^2$, and thus $\sigma_s(1) = 2$. Along the same lines we can obtain the moments of the avalanche time distribution. In this case, $\langle t^q \rangle_L \sim L^{\sigma_t(q)}$, with $\partial\sigma_t(q)/\partial q = z$. Analogous considerations for small q apply also for the time moment analysis. Then, the τ_t exponent can be found using the scaling relation $z(2 - \tau_t) = \sigma_t(1)$.

We have computed the exponents τ_s, τ_t, D, and z from our data, using the moment analysis method. Our results are reported in Tables 1 and 2. The validity of these exponents can be checked *a posteriori* by means of a data collapse analysis: If the FSS hypothesis of equations (3) and (4) is correct, then the plots of the distributions, under the rescaling $s \to s/L^D$ and $P(s) \to P(s)L^{D\tau_s}$, and correspondingly $t \to t/L^z$ and $P(t) \to P(t)L^{z\tau_t}$, should collapse onto the same universal function, for different values of L. Figures 2 and 3 show the data collapse for the distributions of sizes and times in $d = 2$, respectively. Analogous plots for the case $d = 3$ are presented in Figures 4 and 5. From these plots we conclude that our model fulfills the FSS hypothesis, and is in this sense critical, being characterized by the exponents reported in Tables 1 and 2.

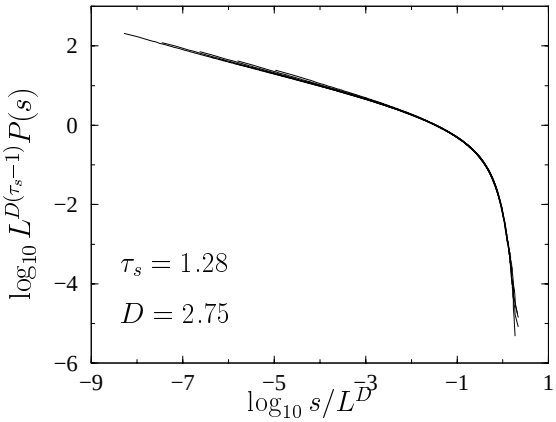

Fig. 2. Data collapse analysis of the integrated avalanche size distribution for the conserved RD model in $d = 2$. System sizes $L = 64, 128, 256, 512,$ and 1024.

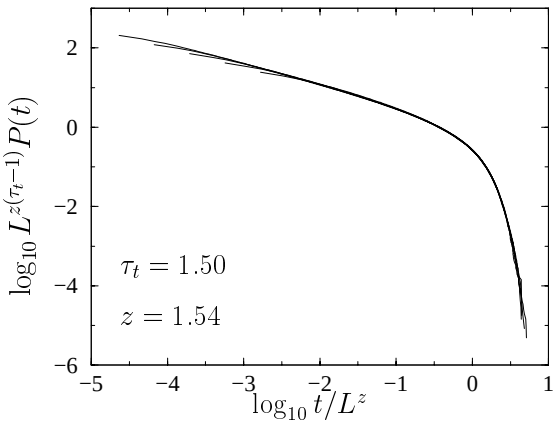

Fig. 3. Data collapse analysis of the integrated avalanche time distribution for the conserved RD model in $d = 2$. System sizes $L = 64, 128, 256, 512,$ and 1024.

Once we have shown that the slowly driven conserved RD model exhibits SOC behavior, it is interesting to check whether it shares the same universality class with any other SOC models. Given its stochastic rules, the natural candidate for comparison is the stochastic Manna sandpile model [8,16]. In Table 1 we quote the exponents for the Manna model in $d = 2$, whose value has been relatively well established by different sets of independent

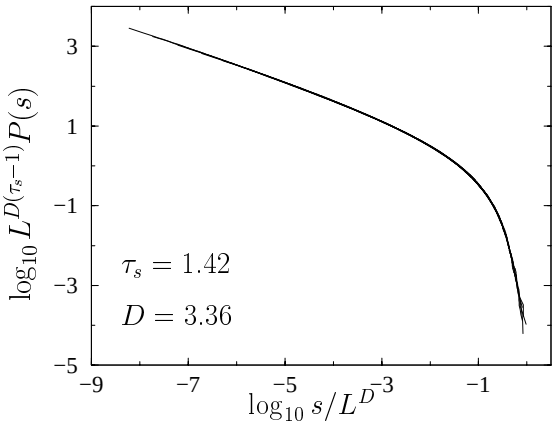

Fig. 4. Data collapse analysis of the integrated avalanche size distribution for the conserved RD model in $d = 3$. System sizes $L = 74, 100, 140, 200,$ and 280.

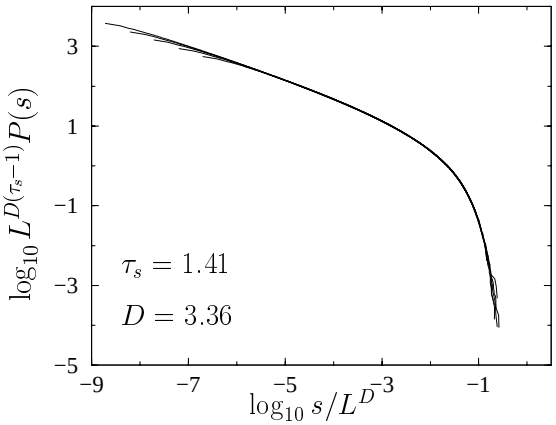

Fig. 6. Data collapse analysis of the integrated avalanche size distribution for the stochastic Manna model in $d = 3$. System sizes $L = 100, 140, 200, 280,$ and 400.

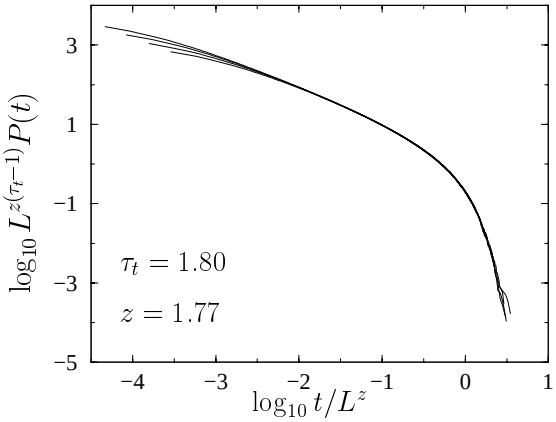

Fig. 5. Data collapse analysis of the integrated avalanche time distribution for the conserved RD model in $d = 3$. System sizes $L = 100, 140, 200,$ and 280.

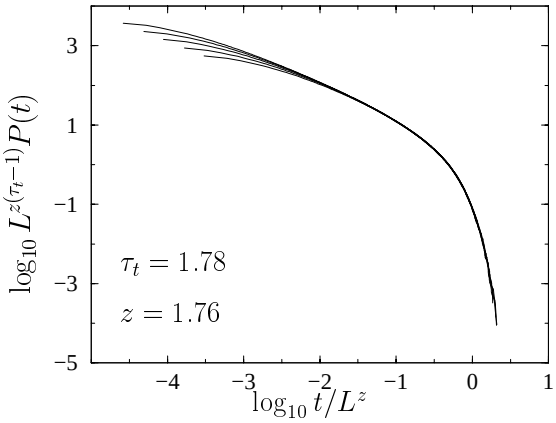

Fig. 7. Data collapse analysis of the integrated avalanche time distribution for the stochastic Manna model in $d = 3$. System sizes $L = 100, 140, 200, 280,$ and 400.

simulations [17–20]. The case $d = 3$ has not been studied so thoroughly, with the exception of the simulations of Lübeck [18]. Thus, in order to compare our results with the conserved RD model, we have carried out large-scale simulations of the $d = 3$ stochastic Manna model. The exponents obtained are given in Table 2, while Figures 6 and 7 plot the data collapse for sizes and times, respectively. Averages are performed over 10^7 non-zero avalanches, and the system sizes considered range from $L = 74$ to $L = 400$ (larger than those achieved by Lübeck [18]).

From the examination of Tables 1 and 2, we conclude that the present conserved RD model exhibits exponents fully compatible with those of the stochastic Manna sandpile model in both $d = 2$ and $d = 3$. This coincidence of exponents proves that both models belong to the same universality class. This fact is altogether not surprising, since both models exhibit the same basic symmetries: isotropic diffusion of particles, stochastic conserved microscopic rules, and presence of infinitely many – in the thermodynamic limit – absorbing states. This result represents a further confirmation of the universality claim made in references [12,13] for this kind of systems.

In summary, we have shown how to construct a slowly-driven conserved RD system which exhibits SOC behavior (avalanche macroscopic dynamics). The key points are the application of the slow-driving condition (addition of new B particles) plus boundary dissipation (diffusion of B particles out of the system). The model is characterized by critical exponents that place it in the same universality class than the Manna stochastic sandpile model. The related model proposed in reference [11] with $D_A \neq 0$, however, belongs to a different universality class [12]. The limit $D_A \to 0$ in the theory with $D_A \neq 0$ is non-analytic; any infinitesimal amount of diffusion in the energy field renormalizes to a finite value, and definitely changes the universality class of the model.

This work has been supported by the European Network under Contract No. ERBFMRXCT980183. RP-S also acknowledges support from the grant CICYT PB97-0693.

References

1. P. Bak, C. Tang, K. Wiesenfeld, Phys. Rev. Lett. **59**, 381 (1987).
2. H.J. Jensen, *Self-Organized Criticality* (Cambridge University Press, Cambridge, 1998).
3. R. Dickman, A. Vespignani, S. Zapperi, Phys. Rev. E **57**, 5095 (1998); A. Vespignani, R. Dickman, M.A. Muñoz, S. Zapperi, Phys. Rev. Lett. **81**, 5676 (1998).
4. A. Vespignani, R. Dickman, M.A. Muñoz, S. Zapperi, Phys. Rev. E **62**, 4564 (2000).
5. R. Dickman, M.A. Muñoz, A. Vespignani, S. Zapperi, Braz. J. Phys. **30**, 27 (2000).
6. G. Grinstein, in *Scale Invariance, Interfaces and Nonequilibrium Dynamics*, *NATO Advanced Study Institute, Series B: Physics*, Vol. 344, edited by A. McKane *et al.* (Plenum, New York, 1995).
7. Y.-C. Zhang, Phys. Rev. Lett. **63**, 470 (1989).
8. S.S. Manna, J. Phys. A **24**, L363 (1991).
9. B. Drossel, F. Schwabl, Phys. Rev. Lett. **69**, 1629 (1992).
10. P. Bak, K. Sneppen, Phys. Rev. Lett. **71**, 4083 (1993).
11. F. van Wijland, K. Oerding, H.J. Hilhorst, Physica A **251**, 179 (1998).
12. R. Pastor-Satorras, A. Vespignani, Phys. Rev. E **62**, R5875 (2000).
13. M. Rossi, R. Pastor-Satorras, A. Vespignani, Phys. Rev. Lett. **85**, 1803 (2000).
14. *Finite Size Scaling*, Vol. 2 of *Current Physics-Sources and Comments*, edited by J.L. Cardy (North Holland, Amsterdam, 1988).
15. M. De Menech, A.L. Stella, C. Tebaldi, Phys. Rev. E **58**, R2677 (1998); C. Tebaldi, M. De Menech, A.L. Stella, Phys. Rev. Lett **83**, 3952 (1999).
16. D. Dhar, Physica A **263**, 4 (1999).
17. A. Chessa, A. Vespignani, S. Zapperi, Comput. Phys. Commun. **121-122**, 299 (1999).
18. S. Lübeck, Phys. Rev. E **61**, 204 (2000).
19. K. Nakanishi, K. Sneppen, Phys. Rev. E **55**, 4012 (1997).
20. E. Milshtein, O. Biham, S. Solomon, Phys. Rev. E **58**, 303 (1998).